AIAA JOURNAL
Vol. 45, No. 3, March 2007

Elastic Buckling and Imperfection Sensitivity of Generally Stiffened Conical Shells

Yiska Goldfeld*
Technion-Israel Institute of Technology, 32000 Haifa, Israel

DOI: 10.2514/1.25830

The sensitivity of stiffened conical shells to imperfection is considered, via the initial postbuckling analysis. Unlike stiffened cylindrical shells, in the case of stiffened conical shells the stiffeners' inclination and the distance between the stiffeners vary with the shell coordinates, which complicates the problem considerably. The main objective of the study is to investigate the influence of the stiffeners on the buckling load and on the imperfection sensitivity. It is felt that by finding the various parameters that influence the shell's imperfection sensitivity, it is possible to improve the behavior of the whole structure. A special computer code had been developed to calculate the classical buckling load and the imperfection sensitivity via Koiter's theory of generally stiffened conical shells with consideration to the variation of the material properties in the shell's coordinates. In the present work the shell is assumed to be closely stiffened and a smeared approach is adopted. Therefore, only global buckling behavior is considered.

Nomenclature

$\boldsymbol{A}$ = membrane stiffness coefficients
a = Koiter's sensitivity parameter
a_{11} = contribution of the stiffeners to the membrane stiffness, Eq. (7)
$\boldsymbol{B}$ = coupling stiffness coefficients
b = Koiter's sensitivity parameter
b_1 = distance between the stiffeners for $x = 0$
b_{11} = contribution of the stiffeners to the coupling stiffness, Eq. (7)
$b(x)$ = general distance between stiffeners
C = $\cos(\beta)$
$\boldsymbol{D}$ = flexural stiffness coefficients
d_{11}, d_{66} = contribution of the stiffeners to the flexular stiffness, Eq. (7)
E = elastic moduli
$\boldsymbol{J}_1, \boldsymbol{J}_2$ = transformation matrices, Eqs. (9) and (14)
L = slant length of the conical shell
$\boldsymbol{L}_1, \boldsymbol{L}_2$ = transformation matrices, Eqs. (10) and (15)
$\boldsymbol{M}$ = moment resultants $\{M_{xx}, M_{\theta\theta}, M_{x\theta}\}$
$\boldsymbol{N}$ = force resultants $\{N_{xx}, N_{\theta\theta}, N_{x\theta}\}$
N_{xxcr} = axial compression buckling load
p_{cr} = hydrostatic buckling load
R_1 = radius at the narrower end of the cone
$R(x)$ = radius at x-coordinate
S = $\sin(\beta)$
u = in-plane longitudinal displacement
v = in-plane circumferential displacement
w = radial displacement (positive inward)
x = axial coordinate for conical shell (see Fig. 1)
z = coordinate perpendicular to the shell wall (positive inward)
α = cone semivertex angle
β_1 = stiffeners' inclination at $x = 0$
$\beta(x)$ = stiffeners' inclination, Eq. (11)
$\boldsymbol{\varepsilon}$ = strains $\{\varepsilon_{xx}, \varepsilon_{\theta\theta}, \gamma_{x\theta}\}$
$\boldsymbol{\varepsilon}^0$ = strains at the reference surface $\{\varepsilon^0_{xx}, \varepsilon^0_{\theta\theta}, \gamma^0_{x\theta}\}$
θ = circumferential coordinate
ν = Poisson's ratio
$\boldsymbol{\chi}$ = change of curvature and twist of the middle surface $\{\chi_{xx}, \chi_{\theta\theta}, \chi_{x\theta}\}$

Presented as Paper 2275 at the 47th AIAA/ASME/ASCE/AHS/ASC Structures, Structural Dynamics, and Materials Conference, Newport, RI, 1–4 May 2006; received 13 June 2006; revision received 31 August 2006; accepted for publication 26 September 2006.

*Senior Lecturer, Faculty of Civil and Environmental Engineering; yiska@tx.technion.ac.il. Member AIAA.

Introduction

SHELL structures are widely used in aeronautic, marine, and civil engineering structures; they belong to the thin-wall structure family, which are very sensitive to imperfection; and their sensitivity depends on the geometry of the shell and its mechanical properties. One of the main goals, in this field, is to find the various parameters that influence the shell's sensitivity, thus to improve the behavior of the whole structure. One of the ways to increase the buckling load and to decrease the sensitivity to imperfection as well is to add stiffeners to the shell structure. However, adding stiffeners to the shell structures must be done with strict attention, because adding stiffeners incorrectly would, in some cases, not change the behavior of the shell at all.

Conical shells are usually used as a connection between two cylindrical shells with different diameters. Unlike stiffened cylindrical shell, in the case of stiffened conical shells the distance between the stiffeners and the angle of inclination of the stiffeners varies with the shell coordinates, which ultimately results in coordinate dependence of the contribution to the stiffness coefficients of the $\boldsymbol{A}$, $\boldsymbol{B}$, and $\boldsymbol{D}$ matrices. This effect complicates the problem considerably. The first level of complexity is attributed to the need to find an analytical representation of the variation of the material properties. A thorough study of the stiffness functions and their dependence on many factors has been performed by Baruch et al. [1]. The second level of complexity is associated with the introduction of coordinate dependent stiffness matrices into the mathematical model and the solution of the system of nonlinear governing partial differential equations with variable coefficients. In earlier investigations (Baruch et al. [2], Baruch and Singer [3], and Shalev et al. [4]) the stiffeners were considered as stringers (positioned in the axial direction, the distance between the stringers varies linearly) or as rings (positioned in circumferential direction, equally distributed). Other investigators (Chryssanthopoulos and Spagonali [5], Spagonli and Chryssanthopoulos [6]) used finite elements commercial computer code to solve the buckling and postbuckling behavior of stringer-stiffened conical shells.

This work presents a qualitative study of the imperfection-sensitivity of eccentrically stiffened conical shells in a general direction, by consideration of the variation of the stiffness coefficients and their dependence on the shell's coordinate. In the present work the shell is assumed to be closely stiffened, and a "smeared" approach is adopted, see Baruch and Singer [7]. Therefore, there is no possibility of local buckling between stiffeners and only global buckling behavior is considered. Investigation is made within the framework of Koiter's general theory of postbuckling behavior [8]. The calculations provide a measure of the extent to which the shells are sensitive or insensitive to imperfections in their shape and thus indicate to what extent the classical buckling results can be reliable.

The main objective of the study is to investigate the influence of the stiffeners on the characteristic buckling behavior and on the imperfection sensitivity of generally stiffened conical shells, taking into account the variation of the material properties with the shell's coordinates. It is felt that by finding the various parameters that influence the shell's imperfection sensitivity, it is possible to improve the behavior of the whole structure. Moreover, the objective is to investigate the influence of the variation of the stiffness coefficients on the characteristic behavior of the shell, to find a simple estimate to the exact solution (taking into account the variation of the material properties). Therefore, a comparison with the solution derived by nominal material properties (taken from the midlength of the shell and assumed to be constant all over the shell surface) will be carried out.

The nonlinear equilibrium differential equations are derived from the basis of their kinematic approach, using the displacement components (axial u, circumferential v, and normal w) as the unknown dependent variables. The asymptotic technique is used to convert the nonlinear equations into three linear sets. These equations are solved through expansion of the dependent variables in Fourier series in the circumferential direction and in finite differences in the axial direction. Afterwards the Galerkin procedure is used to minimize the error due to the truncated form of the series. A special computer code was developed and used for a wide range of parametric study of buckling and sensitivity behavior of generally stiffened conical shells.

Governing Equation

This solution procedure has been used before by Goldfeld et al. [9] for isotropic conical shells, and by Goldfeld and Arbocz [10] for the buckling of laminated conical shell. For the imperfection sensitivity of stiffened cones some additional complications occur.

Kinematics Relation: Donnell's Theory [11]

The strain-displacement relation can be written as

$$\{\boldsymbol{\varepsilon}\} = \{\boldsymbol{\varepsilon}^0\} + z\{\boldsymbol{\chi}\} \tag{1}$$

where $\{\boldsymbol{\varepsilon}^0\}$ and $\{\boldsymbol{\chi}\}$ are, respectively, the strain and change-of-curvature vectors of the reference surface, composed as follows, see Goldfeld et al. [9]:

$$\begin{aligned}
\varepsilon_{xx}^0 &= u_{,x} + \frac{1}{2}w_{,x}^2 \\
\varepsilon_{\theta\theta}^0 &= \frac{v_{,\theta}}{r(x)} + \frac{w}{r(x)}\cos(\alpha) + \frac{u}{r(x)}\sin(\alpha) + \frac{w_{,\theta}^2}{2r(x)^2} \\
\gamma_{x\theta}^0 &= \frac{u_{,\theta}}{r(x)} + v_{,x} - \frac{v}{r(x)}\sin(\alpha) + \frac{w_{,x}w_{,\theta}}{r(x)}
\end{aligned} \tag{2}$$

$$\begin{aligned}
\chi_{xx} &= -w_{,xx} \qquad \chi_{\theta\theta} = -\frac{w_{,\theta\theta}}{r(x)^2} - \frac{w_{,x}}{r(x)}\sin(\alpha) \\
\chi_{x\theta} &= -\frac{w_{,x\theta}}{r(x)} - \frac{w_{,\theta}}{r(x)^2}\sin(\alpha)
\end{aligned} \tag{3}$$

where $(\,)_{,x}$ and $(\,)_{,\theta}$ denote the derivatives with respect to the axial (x) and circumferential (θ) coordinate, respectively (see Fig. 1).

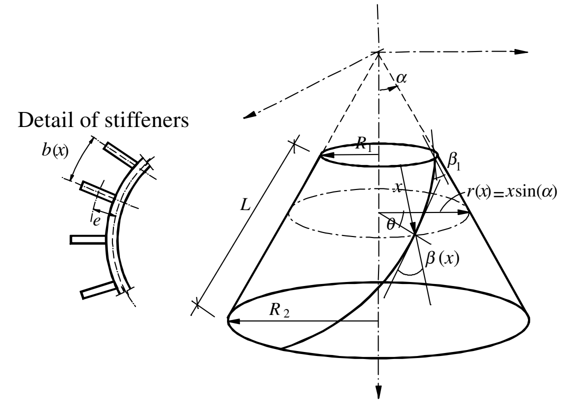

Fig. 1 Geometry, sign conventions for the coordinates, and the position of the stiffener on a conical shell.

Constitutive Equations: Stiffened Conical Shells

Under the classical laminate theory, Jones [12] and Whitney [13], the constitutive equation reads

$$\begin{Bmatrix} \boldsymbol{N} \\ \boldsymbol{M} \end{Bmatrix} = \begin{bmatrix} \boldsymbol{A} & \boldsymbol{B} \\ \boldsymbol{B} & \boldsymbol{D} \end{bmatrix} \begin{Bmatrix} \boldsymbol{\varepsilon}^0 \\ \boldsymbol{\chi} \end{Bmatrix} \tag{4}$$

where $\{\boldsymbol{N}\}^T = \{N_{xx}, N_{\theta\theta}, N_{x\theta}\}$ and $\{\boldsymbol{M}\}^T = \{M_{xx}, M_{\theta\theta}, M_{x\theta}\}$ are the force and moment resultants vectors, $\{\boldsymbol{\varepsilon}^0\}^T = \{\varepsilon_{xx}^0, \varepsilon_{\theta\theta}^0, \varepsilon_{x\theta}^0\}$ and $\{\boldsymbol{\chi}\}^T = \{\chi_{xx}, \chi_{\theta\theta}, \chi_{x\theta}\}$ are the strain at the reference surface and the change of curvature and twist of the middle surface, respectively.

The present work allows for both internally and externally eccentric stiffener in a general position. The shell is assumed to be closely stiffened. Therefore, there is no possibility of local buckling between stiffeners and it is possible to "smear" the stiffeners (Baruch and Singer [7]), so the stress resultants and moment per unit length are given by

$$N_{ij} = N_{ij}^{\text{shell}} + N_{ij}^{\text{stiff}} \qquad M_{ij} = M_{ij}^{\text{shell}} + M_{ij}^{\text{stiff}} \tag{5}$$

where N_{ij}^{shell} and M_{ij}^{shell} are the stress resultants and couples per unit length of the shells' sheet. N_{ij}^{stiff} and M_{ij}^{stiff} are the stiffeners' contributions to the load carrying capacity of the shell (per unit length). These contributions are based on the following assumptions regarding the constitutive relations (Baruch et al. [1], Baruch and Singer [7]):

1) The stiffeners are made of isotropic material with linear elastic behavior.

2) The stiffeners can be positioned in any direction and are distributed mathematically, for calculation purposes, over the whole surface of the shell.

3) The stiffener-laminate connection is monolithic, hence the normal strains (ε_{zz}) vary linearly in the stiffener as well as in the sheet and equal at their point of contact.

4) The stiffeners do not transmit shear perpendicular to their axes.

5) The stiffener resists torsion due to its torsional rigidity.

As a result of these assumptions the internal forces and moments about the surface of reference, due to the stiffeners only, are obtained as functions of the strains and the curvatures of the reference surface in the direction of the stiffeners (1, 2).

$$N_1 = a_{11}\varepsilon_1^0 + b_{11}\chi_1 \qquad M_1 = b_{11}\varepsilon_1^0 + d_{11}\chi_1 \qquad M_{12} = d_{66}\chi_{12} \tag{6}$$

where

$$\begin{aligned}
a_{11} &= \frac{E_{\text{st}}A_{\text{st}}}{b(x,\theta)} \qquad b_{11} = \frac{E_{\text{st}}A_{\text{st}}e}{b(x,\theta)} \qquad d_{11} = \frac{E_{\text{st}}(I_{\text{st}} + A_{\text{st}}e^2)}{b(x,\theta)} \\
d_{66} &= \frac{1}{4}\frac{G_{\text{st}}I_{\text{tst}}}{b(x,\theta)}
\end{aligned} \tag{7}$$

E_{st} is the modulus of elasticity of the stiffener, G_{st} is the shear modulus of elasticity of the stiffener, A_{st} is the cross-sectional area of the stiffener, e is the distance of the centroid of the stiffener cross section from the surface of reference, I_{st} is the moment of inertia of the stiffener cross section about itself, and I_{tst} is the torsion constant of the stiffener cross section. b is the distance between the stiffeners, and for a generally stiffened conical shell it depends on the shell's coordinates, $b(x, \theta)$. For optimization purpose the geometrical characteristics of the cross section of the stiffeners can be chosen to be also some function of x and θ. Therefore, a_{11}, b_{11}, d_{11}, and b_{66} are strong functions of the shell's coordinate.

Under the classical laminate theory, the contribution of the stiffeners to stiffness matrices expressed in the basic coordinates system of the shell (x, θ) is given by

$$\boldsymbol{A}^{\text{stiff}} = a_{11}\boldsymbol{J}_1 \qquad \boldsymbol{B}^{\text{stiff}} = b_{11}\boldsymbol{J}_1 \qquad \boldsymbol{D}^{\text{stiff}} = d_{11}\boldsymbol{J}_1 + d_{66}\boldsymbol{L}_1 \tag{8}$$

where

$$\boldsymbol{J}_1 = \begin{bmatrix} C^4 & C^2S^2 & C^3S \\ C^2S^2 & S^4 & CS^3 \\ C^3S & CS^3 & C^2S^2 \end{bmatrix} \tag{9}$$

$$\boldsymbol{L}_1 = \begin{bmatrix} 4C^2S^2 & -4C^2S^2 & -2CS(C^2 - S^2) \\ -4C^2S^2 & 4C^2S^2 & 2CS(C^2 - S^2) \\ -2CS(C^2 - S^2) & 2CS(C^2 - S^2) & (C^2 - S^2)^2 \end{bmatrix} \tag{10}$$

where $C = \cos[\beta(x, \theta)]$ and $S = \sin[\beta(x, \theta)]$; β is the angle of inclination of the stiffeners and is a function of x and θ, which depends on the chosen position of the stiffeners.

In this work a geodesic path (the shortest distance between two points on a surface) is chosen to represent the variation of the stiffeners in the shell's coordinate; therefore the stiffeners' inclination β and the distance between the stiffeners b changes only in the axial direction and is constant in the circumferential direction. A geodesic path is commonly used when laminated conical shells are produced by a filament winding process when there is no friction between the fiber and the cone mandrel. The same procedure can be used when stiffened isotopic cones and stiffened laminated cones are produced. The stiffeners' inclination $\beta(x)$ is given by

$$\beta(x) = \arcsin\left(\frac{R_1 \sin\alpha}{x + R_1 \sin\alpha} \sin\beta_1\right) \tag{11}$$

where β_1 is the stiffener inclination at the small end of the shell and x is the longitudinal coordinate in the cone surface, see Fig. 1.

The distance between the stiffeners $b(x)$ is given by

$$b(x) = b_1 \frac{(x + R_1 \sin\alpha)\cos\beta}{R_1 \sin\alpha \cos\beta_1} \tag{12}$$

where b_1 is the distance between the fibers at the narrower edge of the cone.

Therefore, the stiffness matrices $\boldsymbol{A}^{\text{stiff}}$, $\boldsymbol{B}^{\text{stiff}}$, and $\boldsymbol{D}^{\text{stiff}}$, are strong functions of the longitudinal coordinate and have to be added to the stiffness matrices given by the shell's sheet. Note that for $\beta = 0$ one obtains the case of stringers (contribution to the stiffness coefficients A_{11}, B_{11}, and D_{11}, which vary linearly along the axial direction). In the case of a stiffener orientation of $\beta = \pi/2$ the assumption of a geodesic path is not valid. The stiffener inclination and the distance between stiffeners remain constant along the axial direction and the buckling load and the initial postbuckling behavior can be calculated on the basis of constant stiffness coefficients. In this case $(\beta = \pi/2)$, one obtains the case of ring stiffeners (constant contribution to the stiffness coefficients A_{22}, B_{22}, and D_{22}).

In Fig. 2 the change of the stiffener inclination and the distance between the stiffeners are plotted vs the longitudinal coordinate for conical shell (with cone semivertex angle of $\alpha = 45$ deg, a slant length of $L = 2.54$ m, and the small radius of the cone $R_1 = 1.27$ m) with various initial stiffeners inclination (β_1). It is seen that the stiffener inclination decreases along the axial direction, the distance between stiffeners increases along the axial direction, and the higher the initial stiffener inclination the more rapid the change along the axial direction.

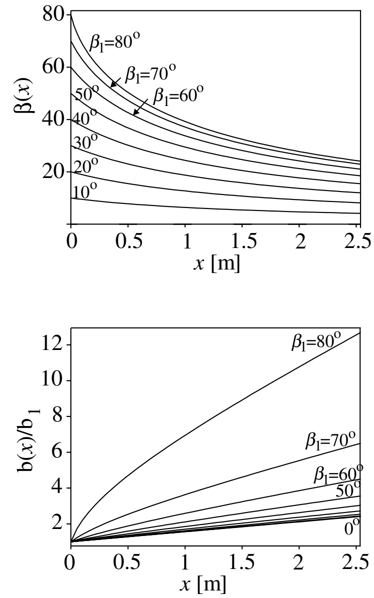

Fig. 2 Variation of the stiffener's inclination and the distance between stiffeners vs the cone slant length for conical shell $\alpha = 45$ deg.

For a general angle of inclination β, the stiffening of the stiffeners will be "unbalanced." To have balanced stiffening one must add the same stiffeners with an angle of inclination $-\beta$. For this case one obtains

$$\boldsymbol{A}^{\text{stiff}} = 2a_{11}\boldsymbol{J}_2 \qquad \boldsymbol{B}^{\text{stiff}} = 2b_{11}\boldsymbol{J}_2 \qquad \boldsymbol{D}^{\text{stiff}} = 2d_{11}\boldsymbol{J}_2 + 2d_{66}\boldsymbol{L}_2 \tag{13}$$

where the balanced matrices $\boldsymbol{J}_2$ and $\boldsymbol{L}_2$ are given by

$$\boldsymbol{J}_2 = \begin{bmatrix} C^4 & C^2S^2 & 0 \\ C^2S^2 & S^4 & 0 \\ 0 & 0 & C^2S^2 \end{bmatrix} \tag{14}$$

$$\boldsymbol{L}_2 = \begin{bmatrix} 4C^2S^2 & -4C^2S^2 & 0 \\ -4C^2S^2 & 4C^2S^2 & 0 \\ 0 & 0 & (C^2 - S^2)^2 \end{bmatrix} \tag{15}$$

It must be emphasized that for cylindrical shell, the stiffness coefficients, due to the stiffeners with constant geometrical characteristics, will become automatically constants.

Equilibrium Equations

The nonlinear equilibrium equations and the appropriate boundary conditions are derived on the basis of the stationary potential energy criterion. The following set of nonlinear equilibrium equations are obtained as

$$N_{xx,x} + \frac{N_{x\theta,\theta}}{r(x)} + \frac{\sin(\alpha)}{r(x)}[N_{xx} - N_{\theta\theta}] + q_u = 0 \tag{16a}$$

$$N_{x\theta,x} + \frac{N_{\theta\theta,\theta}}{r(x)} + \frac{2\sin(\alpha)}{r(x)}N_{x\theta} + q_v = 0 \tag{16b}$$

$$M_{xx,xx} + \frac{M_{\theta\theta,\theta\theta}}{r(x)^2} + \frac{2M_{x\theta,x\theta}}{r(x)} - \frac{N_{\theta\theta}}{r(x)}\cos(\alpha) + \frac{\sin(\alpha)}{r(x)}\left[2M_{xx,x} - M_{\theta\theta,x} + \frac{2M_{x\theta,\theta}}{r(x)}\right] + \frac{1}{r(x)}[r(x)N_{xx}w_{,x} + N_{x\theta}w_{,\theta}]_{,x} + \frac{1}{r(x)}\left[N_{x\theta}w_{,x} + \frac{N_{\theta\theta}w_{,\theta}}{r(x)}\right]_{,\theta} + q_w = 0 \tag{16c}$$

with the following boundary conditions:

$$N_{xx} = \bar{N}_{xx} \quad \text{or} \quad u = \bar{u}, \qquad N_{x\theta} = \bar{N}_{x\theta} \quad \text{or} \quad v = \bar{v},$$
$$M_{xx,x} + \frac{2M_{x\theta,\theta}}{r(x)} + N_{xx}w_{,x} + \frac{N_{x\theta}w_{,\theta}}{r(x)} + \frac{\sin(\alpha)}{r(x)}(M_{xx} - M_{\theta\theta})$$
$$= \bar{Q} \quad \text{or} \quad w = \bar{w}$$
$$M_{xx} = \bar{M}_{xx} \quad \text{or} \quad w_{,x} = \bar{w}_{,x} \tag{17}$$

where q_u, q_v, and q_w are the external distributed loading in the axial, circumferential, and normal directions, respectively. $\bar{N}_{xx}$, $\bar{N}_{x\theta}$, $\bar{Q}$, and $\bar{M}_{xx}$ are, respectively, the axial, torsional, shearing forces, and the bending moment through the boundaries. It must be mentioned that for practical applications a "ring" boundary conditions (corresponding to zero normal-to-cone-axes displacements) are used for conical shells, see Seide [14], thus $u \sin\alpha + w\cos\alpha = 0$, $v = 0$ (when w is positive outward).

Using Eqs. (2–4) the equilibrium equations in terms of the displacement function read

$$L_h^{[1]}(w) + L_q^{[1]}(v) + L_e^{[1]}(u) + LL_g^{[1]}(w, w)$$
$$+ LL_m^{[1]}(v, v) + LL_n^{[1]}(w, v) + q_u = 0$$
$$L_h^{[2]}(w) + L_q^{[2]}(v) + L_e^{[2]}(u) + LL_g^{[2]}(w, w)$$
$$+ LL_m^{[2]}(v, v) + LL_n^{[2]}(w, v) + LL_s^{[2]}(w, u) + LL_t^{[2]}(u, v)$$
$$+ LLL_p^{[2]}(w, v, w) + LLL_f^{[2]}(v, w, v)$$
$$+ LLL_l^{[2]}(v, v, v) + LLL_y^{[2]}(w, w, w) + q_v = 0$$
$$L_h^{[3]}(w) + L_q^{[3]}(v) + L_e^{[3]}(u) + LL_g^{[3]}(w, w)$$
$$+ LL_n^{[3]}(w, v) + LL_s^{[3]}(w, u) + LLL_y^{[3]}(w, w, w)$$
$$+ LL_m^{[3]}(v, v) + LL_t^{[3]}(u, v) + LLL_p^{[3]}(w, v, w)$$
$$+ LLL_f^{[3]}(v, w, v) + LLL_l^{[3]}(v, v, v) + q_w = 0 \tag{18}$$

$L^{[e]}$, $LL^{[e]}$, and $LLL^{[e]}$, $[e] = 1, 2, 3$, are, respectively, linear, quadratic, and cubic differential operators having variable coefficients. They are given by Sheinman and Goldfeld [15] by

$$L_p^{[e]}(S) = \sum_{i=0}^{4}\sum_{j=0}^{4-i} p_{ij}^{[e]} \frac{\partial^{(i+j)}S}{\partial x^{(i)}\partial\theta^{(j)}} \qquad p = h, q, e \qquad LL_p^{[e]}(S, T) = \sum_{i=0}^{3}\sum_{j=0}^{3-i}\sum_{\ell=0}^{3}\sum_{k=0}^{3-\ell} p_{ijk\ell}^{[e]} \frac{\partial^{(i+j)}S}{\partial x^{(i)}\partial\theta^{(j)}} \frac{\partial^{(\ell+k)}T}{\partial x^{(\ell)}\partial\theta^{(k)}} \qquad p = g, m, n, s, t$$
$$LLL_p^{[e]}(S, T, S) = \sum_{i=0}^{2}\sum_{j=0}^{2-i}\sum_{\ell=0}^{2}\sum_{k=0}^{2-\ell}\sum_{m=0}^{1}\sum_{n=0}^{1-m} p_{ijk\ell mn}^{[e]} \frac{\partial^{(i+j)}S}{\partial x^{(i)}\partial\theta^{(j)}} \frac{\partial^{(\ell+k)}T}{\partial x^{(\ell)}\partial\theta^{(k)}} \frac{\partial^{(m+n)}S}{\partial x^{(m)}\partial\theta^{(n)}} \qquad p = y, l, p, f \tag{19}$$

where $p_{ij}^{[e]}$, $p_{ijk\ell}^{[e]}$ and $p_{ijk\ell mn}^{[e]}$ are, respectively, the coefficients of the elastic parameters. They are functions of $A_{ij}(x)$, $B_{ij}(x)$, $D_{ij}(x)$, and of the radius $r(x)$. S and T are symbolic variables assigned to u, v, and w. Therefore, the coefficients $p_{ij}^{[e]}$, $p_{ijk\ell}^{[e]}$ and $p_{ijk\ell mn}^{[e]}$ are strong functions of the axial coordinate (x), and Eqs. (18) represent a set of nonlinear governing partial differential equations with variable coefficients.

The boundary conditions in terms of the displacement functions are

$$L_{be}^{[1]}(u) + L_{bq}^{[1]}(v) + L_{bh}^{[1]}(w) + LL_{bg}^{[1]}(w, w) + LL_{bm}^{[1]}(v, v) + LL_{bn}^{[1]}(w, v) = \bar{N}_{xx} \quad \text{or} \quad u = \bar{u},$$
$$L_{be}^{[2]}(u) + L_{bq}^{[2]}(v) + L_{bh}^{[2]}(w) + L_{bg}^{[2]}(w, w) + LL_{bm}^{[2]}(v, v) + LL_{bn}^{[2]}(w, v) + LL_{bt}^{[2]}(u, v) + LLL_{bl}^{[2]}(v, v, v)$$
$$+ LLL_{bf}^{[2]}(v, w, v) + LLL_{bp}^{[2]}(w, v, w) = \bar{N}_{x\theta} \quad \text{or} \quad v = \bar{v},$$
$$L_{be}^{[3]}(u) + L_{bq}^{[3]}(v) + L_{bh}^{[3]}(w) + LL_{bg}^{[3]}(w, w) + LL_{bs}^{[3]}(w, u) + LL_{bn}^{[3]}(w, v) + LLL_{by}^{[3]}(w, w, w) + LL_{bm}^{[3]}(u, v)$$
$$+ LL_{bt}^{[3]}(u, v) + LLL_{bp}^{[3]}(w, v, w) + LLL_{bf}^{[3]}(v, w, v) = \bar{Q} \quad \text{or} \quad w = \bar{w},$$
$$L_{b\cdot e}^{[4]}(u) + L_{bq}^{[4]}(v) + L_{bh}^{[4]}(w) + LL_{bg}^{[4]}(w, w) + LL_{bm}^{[4]}(v, v) + LL_{bn}^{[4]}(w, v) = \bar{M}_{xx} \quad \text{or} \quad w_{,x} = \bar{w}_{,x} \tag{20}$$

Buckling and Imperfection Sensitivity Analysis

In Koiter's general theory of elastic stability [8] the imperfection sensitivity of a structure is closely related to its initial postbuckling behavior and the theory is exact in the asymptotic sense. The shape of the secondary equilibrium path plays a central role in determining the influence of initial imperfections. When the initial portion of the secondary path has a positive curvature the structure can develop considerable postbuckling strength, and loss of stability of the primary path does not result in structural collapse. However, when the initial portion of the secondary path has a negative curvature, then in most cases buckling will occur violently and the magnitude of the critical load is subject to the degrading influence of initial imperfections.

The classical buckling load of the perfect structure is denoted by λ_c, and in all cases considered here it is the load at which a nonaxisymmetric bifurcation from the prebuckling state occurs.

Assuming that the eigenvalue problem for the buckling load λ_c will yield a unique buckling mode $\boldsymbol{u}$, a solution to be valid in the initial postbuckling regime is sought in the form of the following asymptotic expansion:

$$\frac{\lambda}{\lambda_c} = 1 + a\xi + b\xi^2 + \cdots$$
$$\begin{Bmatrix} u \\ v \\ w \end{Bmatrix} = \begin{Bmatrix} u^{(0)} \\ v^{(0)} \\ w^{(0)} \end{Bmatrix} + \xi \begin{Bmatrix} u^{(1)} \\ v^{(1)} \\ w^{(1)} \end{Bmatrix} + \xi^2 \begin{Bmatrix} u^{(2)} \\ v^{(2)} \\ w^{(2)} \end{Bmatrix} + \cdots \tag{21}$$

where λ is the load parameter deviating from the bifurcation buckling load λ_c, and ξ is the amplitude of the buckling mode. The superscripts (0), (1), and (2) denote the prebuckling, buckling, and postbuckling states, respectively.

A formal substitution of this expansion into the nonlinear governing Eqs. (18) generates a sequence of equations for the functions appearing in the expansions, whereby the operators used become

$$L(S) = L(S^{(0)}) + \xi L(S^{(1)}) + \xi^2 L(S^{(2)})$$

$$LL(S,T) = LL(S^{(0)},T^{(0)}) + \xi[LL(S^{(0)},T^{(1)}) + LL(S^{(1)},T^{(0)})] + \xi^2[LL(S^{(0)},T^{(2)}) + LL(S^{(2)},T^{(0)}) + LL(S^{(1)},T^{(1)})]$$

$$LLL(S,T,S) = LLL(S^{(0)},T^{(0)},S^{(0)}) + \xi[LLL(S^{(0)},T^{(0)},S^{(1)}) + LLL(S^{(0)},T^{(1)},S^{(0)}) + LLL(S^{(1)},T^{(0)},S^{(0)})] + \xi^2[LLL(S^{(0)},T^{(0)},S^{(2)}) + LLL(S^{(0)},T^{(2)},S^{(0)}) + LLL(S^{(2)},T^{(0)},S^{(0)}) + LLL(S^{(0)},T^{(1)},S^{(1)}) + LLL(S^{(1)},T^{(0)},S^{(1)}) + LLL(S^{(1)},T^{(1)},S^{(0)})] \tag{22}$$

The zeroth-order terms yield the partial differential equations of the prebuckling state:

$$L^{[e]}(S^{(0)}) + LL^{[e]}(S^{(0)},T^{(0)}) + LLL^{[e]}(S^{(0)},T^{(0)},S^{(0)}) = P^{[e]} \qquad e = 1,2,3 \tag{23}$$

The first-order terms yield the partial differential equations of the buckling state:

$$L^{[e]}(S^{(1)}) + [LL^{[e]}(S^{(0)},T^{(1)}) + LL^{[e]}(S^{(1)},T^{(0)})] + [LLL^{[e]}(S^{(1)},T^{(0)},S^{(0)}) + LLL^{[e]}(S^{(0)},T^{(1)},S^{(0)}) + LLL^{[e]}(S^{(0)},T^{(0)},S^{(1)})] = 0 \qquad e = 1,2,3 \tag{24}$$

Finally the second-order terms yield the partial differential equations of the postbuckling state:

$$L^{[e]}(S^{(2)}) + LL^{[e]}(S^{(0)},T^{(2)}) + LL^{[e]}(S^{(2)},T^{(0)}) + LLL^{[e]}(S^{(2)},T^{(0)},S^{(0)}) + LLL^{[e]}(S^{(0)},T^{(2)},S^{(0)}) + LLL^{[e]}(S^{(0)},T^{(0)},S^{(2)}) = LL^{[e]}(S^{(1)},T^{(1)}) + LLL^{[e]}(S^{(1)},T^{(1)},S^{(0)}) + LLL^{[e]}(S^{(0)},T^{(1)},S^{(1)}) + LLL^{[e]}(S^{(1)},T^{(0)},S^{(1)}) \qquad e = 1,2,3 \tag{25}$$

The nonlinear solution of the prebuckling state, Eq. (23), should be performed by an adequate numerical procedure which ultimately yields a limit point. To simplify the problem the solution procedure of the prebuckling state is performed by ignoring the nonlinear terms and solving only the linear part of Eq. (23), that is, $L^{[e]}(S^{(o)}) = P^{[e]}$. The linear solution of the prebuckling state consists of both linear displacement (u, v, w) and linear rotations $(w_{,x}, w_{,\theta})$. The applied loading $P^{[e]}$ consists of axial compression, internal or external pressure, and clockwise or counterclockwise torque. It is assumed to have a uniform spatial distribution and is divided into a fixed part and a variable part. The magnitude of the variable part is allowed to vary in proportion to a load parameter λ. This leads to an eigenvalue problem for the critical load λ_c. Neglecting the nonlinear deformation, that is, essentially using linear prebuckling solution, the equations governing the buckling state, Eqs. (24), become

$$L^{[e]}(S^{(1)} + \lambda_c[LL^{[e]}(S^{(0)},T^{(1)}) + LL^{[e]}(S^{(1)},T^{(0)})] = 0 \qquad e = 1,2,3 \tag{26}$$

where λ_c corresponds to the bifurcation buckling load. These equations admit separable solutions of the form

$$u(x,\theta) = \sum_{m=0}^{2Nu} u_m(x) g_m(\theta) \qquad v(x,\theta) = \sum_{m=0}^{2Nv} v_m(x) g_m(\theta) \qquad w(x,\theta) = \sum_{m=0}^{2Nw} w_m(x) g_m(\theta) \tag{27}$$

where $2N_u$, $2N_v$, and $2N_w$ are the numbers of retained terms in the relevant truncated Fourier series, and

$$g_m(\theta) = \begin{cases} \cos im\theta & m = 0,1,2,3,\ldots,N_3 \\ \sin im\theta & m = N_3+1,\ldots 2N_3 \end{cases} \tag{28}$$

where i denotes the characteristic circumferential wave number. $N_3 = N_u$, or N_v, or N_w, according to the equation number.

The θ-dependence is eliminated by applying Galerkin's procedure. A central finite difference scheme is used to reduce the ordinary differential equations to the following algebraic ones, see Sheinman and Goldfeld [15], Goldfeld et al. [9]:

For the prebuckling state,

$$[\boldsymbol{K}]\{\boldsymbol{Z}^{(0)}\} = \{\boldsymbol{P}\} \tag{29}$$

and for the buckling state,

$$\{[\boldsymbol{K}] + \lambda[\boldsymbol{G}]\}\{\boldsymbol{Z}^{(1)}\} = 0 \tag{30}$$

where $\boldsymbol{K}$ and $\boldsymbol{G}$ are the stiffness and geometry matrices, respectively, and $\boldsymbol{Z}^{(0)}$ and $\boldsymbol{Z}^{(1)}$ are unknown vectors consisting of u, v, w, $u_{,xx}$, $v_{,xx}$, and $w_{,xx}$ for the prebuckling state and the buckling state, respectively. Equation (30) is an eigenvalue problem in which λ represents the buckling load parameters and $\boldsymbol{Z}$ the buckling mode.

Using a linear prebuckling analysis the equations governing the postbuckling state become

$$L^{[e]}(S^{(2)}) + \lambda_c[LL^{[e]}(S^{(0)},T^{(2)}) + LL^{[e]}(S^{(2)},T^{(0)})] + \lambda_c^2[LLL^{[e]}(S^{(2)},T^{(0)},S^{(0)}) + LLL^{[e]}(S^{(0)},T^{(2)},S^{(0)}) + LLL^{[e]}(S^{(0)},T^{(0)},S^{(2)})] = LL^{[e]}(S^{(1)},T^{(1)}) + \lambda_c[LLL^{[e]}(S^{(1)},T^{(1)},S^{(0)}) + LLL^{[e]}(S^{(0)},T^{(1)},S^{(1)}) + LLL^{[e]}(S^{(1)},T^{(0)},S^{(1)})] \qquad e = 1,2,3 \tag{31}$$

$L^{[e]}$, $LL^{[e]}$, $LLL^{[e]}$, S, and T are per Eqs. (18) and (19). The postbuckling state (second-order terms) $w^{(2)}$, $v^{(2)}$, and $u^{(2)}$ are obtained from the solution of the set of three inhomogeneous linear partial differential equations with the associated boundary conditions. The three equilibrium equations and the four boundary conditions for the postbuckling state are given in detail by Goldfeld [16].

These equations admit separable solutions, in the circumferential direction by using Fourier series and the θ-dependence is eliminated by applying Galerkin's procedure, and in the axial direction by using a central finite difference scheme. The ordinary differential equations then reduce to the following algebraic ones:

$$[\boldsymbol{A}]\{\boldsymbol{Z}^{(2)}\} = \{\boldsymbol{F}\} \tag{32}$$

where $\boldsymbol{A}$ and $\boldsymbol{F}$ are the postbuckling matrix and the right-hand side vector, respectively. $\boldsymbol{Z}^{(2)}$ is unknown vectors consisting of $u^{(2)}$, $v^{(2)}$, $w^{(2)}$, $u^{(2)}_{,xx}$, $v^{(2)}_{,xx}$, and $w^{(2)}_{,xx}$ for the postbuckling state.

For perfect shells one is interested in the variation of $\lambda(\xi)$ with ξ in the vicinity of $\lambda = \lambda_c$. Near the bifurcation point λ_c the asymptotic expansion given in Eq. (21) is valid. Because of the periodicity of the buckling mode in the circumferential direction the first postbuckling coefficient a vanishes. For the case of axisymmetric buckling $(n = 0)$ this parameter does not vanish.

For the case of a membrane prebuckling state, Budiansky and Hutchinson [17] derived the well-known formulas

$$a = -\frac{3/2\sigma_1 \cdot L_2(u_2)}{\lambda_c\sigma_0 \cdot L_2(u_1)} \tag{33}$$

$$b = -\frac{\sigma_2 \cdot L_2(u_1) + 2\sigma_1 \cdot L_{11}(u_1,u_2)}{\lambda_c\sigma_0 \cdot L_2(u_1)} \tag{34}$$

For the case of linear prebuckling the following formula is obtained:

$$a = -\frac{3/2\sigma_1 \cdot L_2(u_2)}{\lambda_c[2\sigma_1 \cdot L_{11}(u_0, u_1) + \sigma_0 \cdot L_2(u_1)]} \tag{35}$$

$$b = -\frac{\sigma_2 \cdot L_2(u_1) + 2\sigma_1 \cdot L_{11}(u_1, u_2)}{\lambda_c[2\sigma_1 \cdot L_{11}(u_0, u_1) + \sigma_0 \cdot L_2(u_1)]} \tag{36}$$

By using the orthogonally condition $\sigma_0 L_{11}(u_1, u_n) = 0$ for $n = 0, 2, 3\ldots$ and neglecting the prebuckling deformation $L_{11}(u_0, u_n) = 0$ for $n = 0, 2, 3\ldots$, Eqs. (35) and (36) are degenerated to Eqs. (33) and (34), respectively, obtained by Budiansky and Hutchinson [17].

Cohen [18,19] and Fitch [20] and later on Arbocz and Hol [21,22] calculated Koiter's parameters for the case of nonlinear prebuckling deformation with initial imperfection. Goldfeld [16] presented a short review of the Koiter's parameters obtained by the various assumptions.

For conical shell, with the variables u, v, w the operator will be

$$\sigma_i L_{11}(u_j, u_k) = \int_a^b \int_0^{2\pi} \left\{ N_{xx}^{(i)}[w_{,x}^{(j)} w_{,x}^{(k)}] + N_{\theta\theta}^{(i)}\left[\frac{w_{,\theta}^{(j)} w_{,\theta}^{(k)}}{r(x)^2}\right] + 2N_{x\theta}^{(i)}\left[\frac{w_{,x}^{(j)} w_{,\theta}^{(k)}}{2r(x)} + \frac{w_{,x}^{(k)} w_{,\theta}^{(j)}}{2r(x)}\right]\right\} \mathrm{d}\theta\, \mathrm{d}x \tag{37}$$

$$i, j, k = 0, 1, 2$$

Here, the superscripts (i), (j), and (k) denote the appropriate state [(0)–prebuckling, (1)–buckling, and (2)–initial postbuckling].

Results and Discussion

For the procedure outlined a special computer code, imperfection sensitivity of stiffened conical shells (ISOSCS), was written, covering the buckling and initial postbuckling behavior of generally stiffened conical shells under arbitrary loads and boundary conditions.

Stiffened conical and cylindrical shells under axial compression and under hydrostatic pressure are examined. The geometric properties are: slant length $L = 2.54$ m, the radius at the small end $R_1 = 1.27$ m, and the thickness of the shell's sheet $t = 0.0127$ m ($R_1/t = 100$). The geometric properties of the stiffeners are: the distance between the stiffeners at the small end of the shell $b_1 = 2\pi R_1/30$ (30 stiffeners in the circumferential direction assure that no local buckling will occur), the cross-sectional area of the stiffener $A_{\mathrm{st}} = 0.75 b_1 t$, the moment of inertia of the stiffener cross section about itself $I_{\mathrm{st}} = 50t^3 b_1/12/(1-\nu^2)$, the torsional rigidity of the stiffener cross section is neglected ($I_{\mathrm{tst}} = 0$), and the distance of the centroid of the stiffener cross section from the surface of reference $e = \pm 4.66666t$. For balanced stiffeners configuration $A_{\mathrm{st}}^{\mathrm{balanced}} = A_{\mathrm{st}}/2$ and $I_{\mathrm{st}}^{\mathrm{balanced}} = I_{\mathrm{st}}/2$, thus balanced and unbalanced configurations have the same amount of material. The sheet and the stiffeners are made of isotropic material with material properties as follows: modulus of elasticity $E = 1.404 \times 10^{11}$ N/m^2, Poisson's ratio $\nu = 0.2$.

Axial Compression

The axial compression was applied through the boundary conditions, at the narrower end SS3, that is, $N_{xx} = \bar{N}_{xx}$ and $v = w = M_{xx} = 0$, and at the larger end SS4, that is, $u = v = w = M_{xx} = 0$, where N_{xx} is the axial stress resultant.

Cylindrical Shell

To investigate the influence of the stiffener's inclination, a cylindrical shell with various stiffeners' inclinations is investigated. In this case, the constitutive relations are constant. In Fig. 3 the buckling load and Koiter b-parameter are plotted against the stiffener's inclination. As was expected balanced stiffener configurations give higher buckling load than unbalanced stiffener configurations; however, usually conical shells with balanced stiffener configuration are more sensitive to imperfection than shells with unbalanced configuration. The position of the stiffeners has a significant influence on the buckling load and on the imperfection sensitivity; external stiffeners give higher buckling load but are more sensitive to imperfection than internal stiffeners. Internal stiffeners give relatively lower buckling load but usually assure insensitive shell. Centric stiffeners have no significant advantage compared to the other configuration, especially in the case of balanced configuration (it gives lower buckling load and is also very sensitive to imperfection) because it has kind of orthotropic configuration. The same results were obtained by the classical work of Hutchinson and Amazigo [23] for cylindrical shells with rings and stringer stiffeners under axial compression.

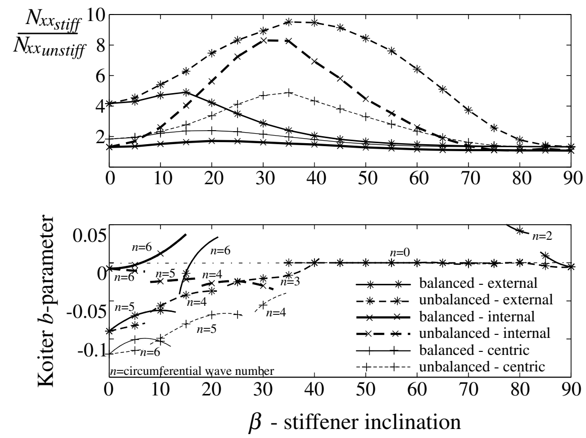

Fig. 3 Normalized axial compressive buckling load and Koiter *b*-parameter vs the stiffener's inclination for cylindrical shell.

For optimization purpose, it seems that the stiffener configuration of $\beta \sim 30$–40 deg for balanced stiffeners and $\beta \sim 15$ deg for unbalanced configuration give the highest buckling loads but are relatively sensitive to imperfection. For unbalanced configuration the circumferential wave number increases until $\beta \sim 30$–35 deg and then decreases. For balanced configuration the circumferential wave number decreases to $n = 0$, axisymmetric buckling. When the buckling behavior is characterized by axisymmetric deformation, the Koiter b-parameter is vanished.

Conical Shell

In Fig. 4 the buckling load and the Koiter b-parameter are plotted against the stiffener's inclination at the small end of the shell (β_1) for conical shell with $\alpha = 45$ deg having different stiffener configurations. The characteristic influence of the stiffeners on the buckling load and imperfection sensitivity parameter is similar to the case of cylindrical shell. In the case of conical shells, stiffener configuration of $\beta_1 \sim 45$ deg for balanced stiffeners and $\beta_1 \sim 0$ deg for unbalanced configuration give the highest buckling load but are quite sensitive to imperfection. The circumferential wave numbers of the balanced configurations are lower than those of the unbalanced configuration.

To try to find a simple estimate for the buckling and the initial postbuckling behavior, comparison with the solution derived by nominal material properties is carried out. Goldfeld and Arbocz [24] found that for laminated conical shells the best estimation to the exact buckling is obtained by taking nominal material properties from the midlength of the shell. In Fig. 5 the buckling load and Koiter b-parameter calculated by varying material properties and nominal ones are given vs the stiffener inclination for conical shell ($\alpha = 45$ deg). The nominal material properties were taken from the midlength of the shell, and are assumed to be constant all over the shell surface. It is seen that the buckling loads are quite different; the buckling loads calculated by varying material properties are higher than the ones calculated by nominal material properties, that is, on the safe side. Not only the buckling load is different, but the buckling

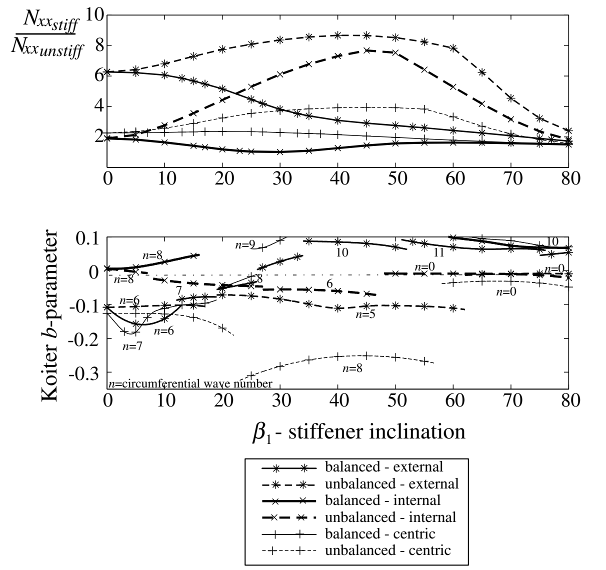

Fig. 4 Normalized axial compressive buckling load and Koiter *b*-parameter vs the stiffener's inclination for conical shell $\alpha = 45$ deg.

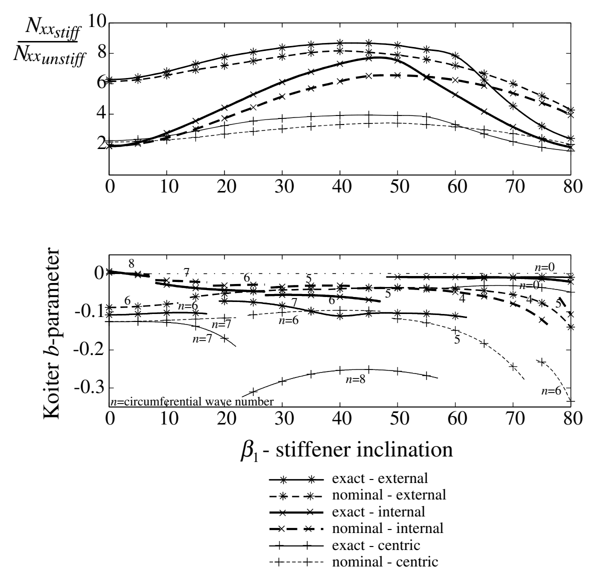

Fig. 5 Normalized axial compressive buckling load and Koiter *b*-parameter vs the stiffener's inclination for conical shell $\alpha = 45$ deg with balanced stiffener configuration calculated by exact and nominal material properties.

mode is too. Usually exact solution of the buckling behavior yields higher circumferential wave numbers than solution based on nominal stiffness, and the deformation mode in the axial direction is different too, see Fig. 6. The differences in the buckling mode affect the initial postbuckling behavior of the shell, and as a result, affect the imperfection sensitivity of the shell. Shells calculated by nominal material properties are less sensitive to imperfection sensitivity. This must be taken into consideration when stiffened conical shells are designed under the assumption that the stiffness coefficients are constant.

In Fig. 7 the buckling load and Koiter *b*-parameter are plotted against the cone semivertex angle for conical shells with initial stiffener inclination of $\beta_1 = 30$ deg at the small end of the shell. Here again, the unbalanced stiffener configurations give lower buckling load but insensitive shells. External stiffeners give higher buckling load but more sensitive shell. Centric stiffeners is the worst configuration for balanced stiffeners; it gives lower buckling load and very sensitive shell. Here again, the circumferential wave numbers of the balanced configurations are lower than those of the

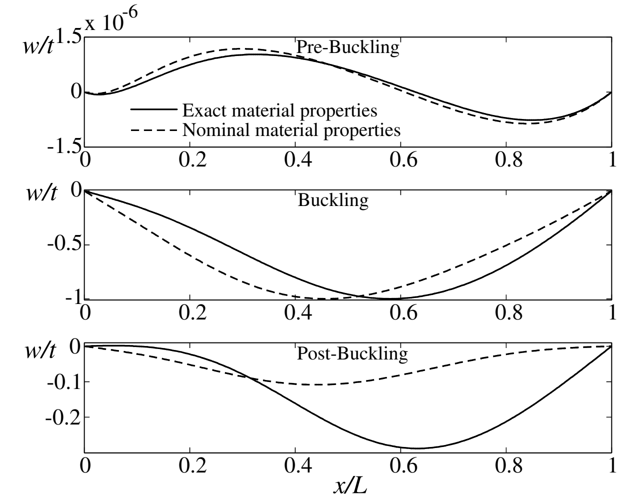

Fig. 6 Prebuckling, buckling mode, initial postbuckling deformations calculated by exact and nominal material properties for conical shell $\alpha = 45$ deg, $\beta_1 = 30$ deg with balanced external stiffener configuration.

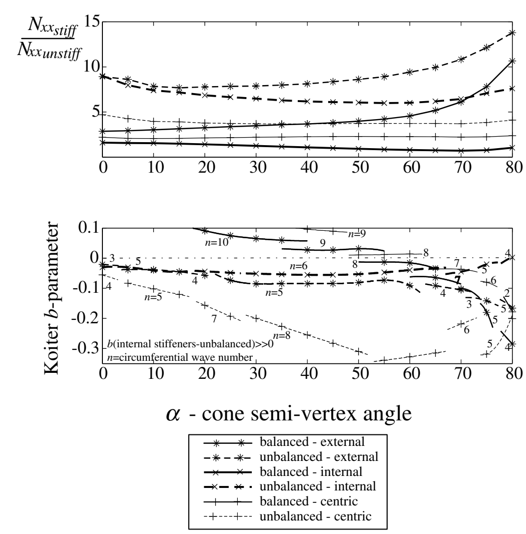

Fig. 7 Normalized axial compressive buckling load and Koiter *b*-parameter vs cone semivertex angle for initial angle of inclination $\beta_1 = 30$ deg.

unbalanced configuration. The higher the cone semivertex angle the lower the buckling load and the more the shell is imperfection sensitive. The reason for that is the variation of the material properties along the longitudinal direction; the higher the cone semivertex angle, the more rapid the variation of the stiffeners along the axial direction.

Hydrostatic Pressure

The hydrostatic pressure was applied to a shell with simply supported boundary conditions (SS4 at both ends, that is, $u = v = w = M_{xx} = 0$).

Cylindrical Shell

In Fig. 8 the buckling load and Koiter *b*-parameter are plotted against the stiffener's inclination, for cylindrical shell (material properties are constant). Similarly to axial compression load case, balanced stiffener configurations give higher buckling load but are more sensitive to imperfection than unbalanced stiffener configurations. The position of the stiffeners has a slight influence on the buckling load and on the imperfection sensitivity, but not in a consistent way. For balanced configuration, internal stiffeners

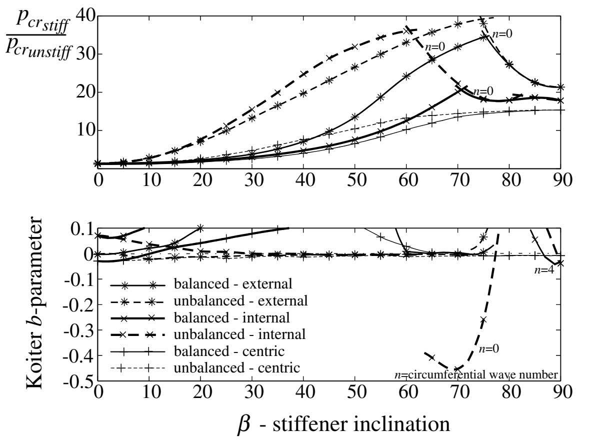

Fig. 8 Normalized buckling load and Koiter *b*-parameter vs the stiffener's inclination for cylindrical shell under hydrostatic pressure.

usually give higher buckling load, and for unbalanced configuration external stiffeners give higher buckling load. Centric stiffeners have no significant advantage compare to the other configuration. The same characteristic behavior was obtained by Hutchinson and Amazigo [23] for cylindrical shells with rings and stringer stiffeners under hydrostatic pressure. Adding stiffeners to the shell almost eliminates the sensitivity to imperfection, except in the case of internal balanced stiffeners when axisymmetric buckling occurs. For optimization purpose, it seems that the stiffener configuration of $\beta \sim 60$–70 deg for balanced stiffeners and $\beta \sim 70$–75 deg for unbalanced configuration give the highest buckling loads. The discontinuity in the slope of the buckling curve occurs at transition from nonaxisymmetric mode to axisymmetric ($n = 0$) mode.

Conical Shell

In Fig. 9 the buckling load and Koiter *b*-parameter are plotted against the stiffener's inclination at the small end of the shell (β_1) for conical shell with $\alpha = 45$ deg having different stiffener configurations. In this case balanced stiffener configurations give much higher buckling load than unbalanced configuration. However, whereas unbalanced stiffener configurations leads to insensitive shell, shells with balanced configuration are sensitive, especially the ones that have external or centric stiffeners. For optimization purpose, stiffener configuration of $\beta_1 \sim 55$ deg for balanced stiffeners and $\beta_1 \sim 65$ deg for unbalanced configuration give the highest buckling load.

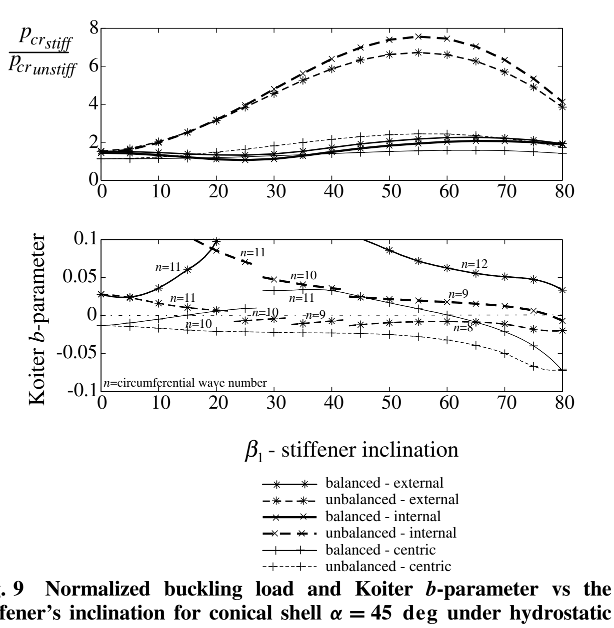

Fig. 9 Normalized buckling load and Koiter *b*-parameter vs the stiffener's inclination for conical shell $\alpha = 45$ deg under hydrostatic pressure.

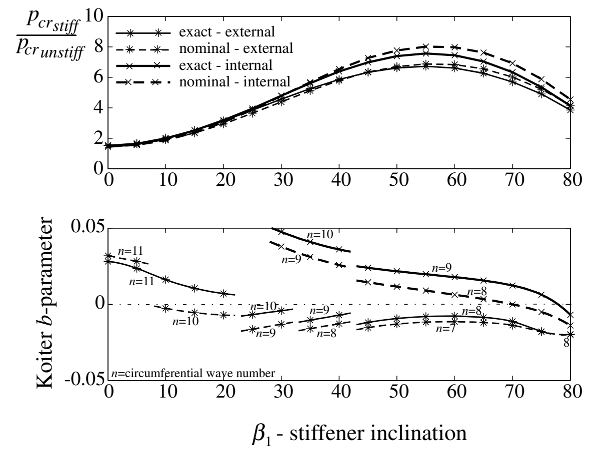

Fig. 10 Normalized buckling load and Koiter *b*-parameter vs the stiffener's inclination for conical shell $\alpha = 45$ deg under hydrostatic pressure with balanced stiffener configuration calculated by exact and nominal material properties.

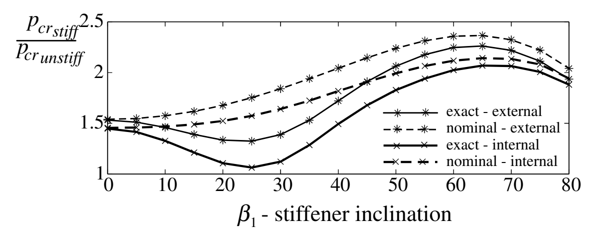

Fig. 11 Normalized buckling load vs the stiffener's inclination for conical shell $\alpha = 45$ deg under hydrostatic pressure with unbalanced stiffener configuration calculated by exact and nominal material properties.

Comparison with the solution derived by the nominal material properties (taken from the midlength of the shell as constant all over the shell surface) is carried out. In Fig. 10 the buckling load and Koiter *b*-parameter calculated by varying material properties and by nominal ones are given vs the stiffener inclination for conical shell ($\alpha = 45$ deg) with balanced configuration. It is seen that in this case, the characteristic buckling behavior calculated by nominal material properties and by exact ones are quite similar. The exact buckling loads are slightly below the nominal ones and the exact sensitivity parameter is slightly above. This is due to the similar characteristic behavior of the buckling mode in the axial direction, which in the case of hydrostatic pressure consists of a half wave. In Fig. 11 the buckling loads calculated by exact material properties and by nominal ones are given for unbalanced configuration. In this case the shell is insensitive to imperfection. Here, the exact buckling loads are below buckling loads calculated by nominal material properties.

Conclusions

In this study, the buckling load and the imperfection sensitivity of a generally stiffened conical shell were investigated under the assumption that stiffener inclination changes as a geodesic path. The improvement in this research is achieved by the adoption of a suitable analytical representation to describe the coordinate dependent stiffness and, especially, by the study of the influence of the variation of the stiffness coefficients on the imperfection sensitivity of the stiffened conical shells.

From the results presented, the following conclusions can be drawn:

1) The position of the stiffeners has a significant influence on the buckling load and on the imperfection sensitivity. Balanced stiffener configurations give higher buckling load but more sensitivity to imperfection. External stiffeners give higher buckling load but are

more sensitive to imperfection than internal stiffeners. Centric stiffeners have no significant improvement for the shells' behavior.

2) The exact buckling behavior differs from the nominal one. Not only the buckling load but also the buckling modes differ, due to the postbuckling behavior, which in turn influences the imperfection sensitivity of the shell.

3) For optimization purpose, to increase the buckling load and to decrease the sensitivity to imperfection, stiffeners should be positioned at $\beta_1 = 50\text{–}60$ deg, depending upon the load case and on the cone semivertex angle.

References

[1] Baruch, M., Arbocz, J., and Zhang, G. Q., "Laminated Conical Shells-Considerations for the Variations of Stiffness Coefficients," Delft University of Technology, Report LR-671, Faculty of Aerospace Engineering, The Netherlands, April 1992.

[2] Baruch, M., Singer, J., and Harari, O., "Generally Instability of Conical Shells with Non-Uniformly Spaced Stiffeners Under Hydrostatic Pressure," *Israel Journal of Technology*, Vol. 3, No. 1, 1965, pp. 62–71.

[3] Baruch, M., and Singer, J., "Generally Instability of Stiffened Circular Conical Shells under Hydrostatic Pressure," *The Aeronautical Quarterly*, May 1965, pp. 187–204.

[4] Shalev, A., Baruch, M., and Nissim, E., "Buckling Analysis of Elastically Constrained Stiffened Conical Shells Under Hydrostatic Pressure by the Collocation Method," *Israel Journal of Technology*, Vol. 11, Nos. 1–2, 1973, pp. 75–87.

[5] Chryssanthopoulos, M. K., and Spagonali, A., "The Influence of Radial Edge Constraint on the Stability of Stiffened Conical Shells in Compression," *Thin-Walled Structures*, Vol. 27, No. 2, 1997, pp. 147–163.

[6] Spagonli, A., and Chryssanthopoulos, M. K., "Buckling Design of Stringer Stiffened Conical Shells in Compression," *Journal of Structural Engineering*, Vol. 125, No. 1, Jan. 1999, pp. 40–48.

[7] Baruch, M., and Singer, J., "Effect of Eccentricity of Stiffeners on the General Instability of Stiffened Cylindrical Shells Under Hydrostatic Pressure," *Journal of Mechanical Engineering Science*, Vol. 5, No. 1, 1963, pp. 23–27.

[8] Koiter, W. T., "The Stability of Elastic Equilibrium," Ph.D. Thesis, H. J. Paris, Delft, Amsterdam, 1945; translated edition, AFFDL, Technical report TR-70-25, Air Force Flight Dynamics Laboratory, Air Force Systems Command, Wright–Patterson AFB, OH, Feb. 1970.

[9] Goldfeld, Y., Sheinman, I., and Baruch, M., "Imperfection Sensitivity of Conical Shell," *AIAA Journal*, Vol. 4, No. 3, 2003, pp. 517–524.

[10] Goldfeld, Y., and Arbocz, J., "Elastic Buckling of Laminated Conical Shells Using a Hierarchical High-Fidelity Analysis Procedure," *Journal of Engineering Mechanics*, 2005 (to be published).

[11] Donnell, L. H., "Stability of Thin-Walled Tubes Under Torsion," NACA TR-479, 1933.

[12] Jones, R. M., *Mechanics of Composite Materials*, McGraw–Hill, New York, 1975.

[13] Whitney, J. M., *Structural Analysis of Laminated Anisotropic Plates*, Technomic, Lancaster, PA, 1987.

[14] Seide, P., "On The Buckling of Truncated Conical Shells Under Uniform Hydrostatic Pressure," *Proceedings of The I.U.T.A.M. Symposium on the Theory of Thin Elastic Shells*, North-Holland Publishing Company, Amsterdam, Holland, 1960, pp. 363–388.

[15] Sheinman, I., and Goldfeld, Y., "Buckling of Laminated Cylindrical Shells in Terms of Different Shell Theories and Formulations," *AIAA Journal*, Vol. 39, No. 9, 2001, pp. 1773–1781.

[16] Goldfeld, Y., "Imperfection Sensitivity of Laminated Conical Shells", *International Journal of Solids and Structures*, 2006 (in press).

[17] Budiansky, B., and Hutchinson, J. W., "Dynamic Buckling of Imperfection Sensitive Structures," *Proceedings of the 11th IUTAM Congress*, Springer–Verlag, Berlin, 1964, pp. 636–651.

[18] Cohen, G. A., "Reply by Author to J. R. Fitch and J. W. Hutchinson," *AIAA Journal*, Vol. 7, No. 7, 1969, pp. 1407–1408.

[19] Cohen, G. A., "Effect of a Nonlinear Prebuckling State on the Postbuckling Behavior and Imperfection Sensitivity of Elastic Structures," *AIAA Journal*, Vol. 6, No. 8, 1968, pp. 1616–1619.

[20] Fitch, J. R., "The Buckling and Postbuckling Behavior of Spherical Caps Under Concentrated Load," *International Journal of Solids and Structures*, Vol. 4, 1968, pp. 421–446.

[21] Arbocz, J., and Hol, J. M. A. M., "Koiter's Stability Theory in a Computer-Aided Engineering (CAE) Environment," *International Journal of Solids and Structures*, Vol. 26, No. 9/10, 1990, pp. 945–973.

[22] Arbocz, J., and Hol, J. M. A. M., "ANILISA—Computational Modules for Koiter's Imperfection Sensitivity Theory," Delft University of Technology, Report LR-582, Faculty of Aerospace Engineering, The Netherlands, 1989.

[23] Hutchinson, J. W., and Amazigo, J. C., "Imperfection Sensitivity of Eccentrically Stiffened Cylindrical Shells," *AIAA Journal*, Vol. 5, No. 3, 1967, pp. 392–401.

[24] Goldfeld, Y., and Arbocz, J., "Buckling of Laminated Conical Shells Given the Variations of the Stiffness Coefficients," *AIAA Journal*, Vol. 42, No. 3, 2004, pp. 642–649.

A. Berman
Associate Editor